International Conference on Space Optics—ICSO 2014

La Caleta, Tenerife, Canary Islands

7–10 October 2014

Instrumental polarization modelling for the PILOT submm experiment

C. Engel

Jean-Philippe Bernard

G. Otrio

Y. Longval

et al.

INSTRUMENTAL POLARIZATION MODELLING
FOR THE PILOT[1] SUBMM EXPERIMENT

C. Engel[1,2,3], J.-Ph Bernard[2,3], †G. Otrio[4], Y. Longval[5], C. Marty[2,3], I. Ristorcelli[2,3]

[1]*Aix Marseille Université, CNRS, LAM (Laboratoire d'Astrophysique de Marseille),*
UMR 7326, Marseille, France
[2]*Université de Toulouse, UPS-OMP, IRAP, F-31028 Toulouse cedex 4, France*
[3]*CNRS, IRAP, 9 Av. colonel Roche, BP 44346, F-31028 Toulouse cedex 4, France*
[4]*CNES, Centre spatial de Toulouse, 18 avenue Edouard Belin, 31401 Toulouse Cedex 9, France*
[5] *Institut d'Astrophysique Spatiale, CNRS (UMR8617) Université Paris-Sud 11, Bâtiment 121, Orsay, France*

I. INTRODUCTION:

A. Context

PILOT [1] is a balloon borne experiment which aims at measuring precisely the polarized emission of the interstellar dust emission, in the submm range (240 and 550 µm). These measurements will be used to reach a better understanding of the galactic magnetic field role in the structure of the Galaxy and the star formation process. They will be useful too for CMB experiments by providing a precise knowledge of galactic foreground emission. Simulations including realistic instrument performances show that after three flights (around 24 hours each), it will be possible to cover the full galactic plane map (±30° in latitude). In addition, several deep surveys will be performed at high galactic latitude. As the level of polarized emission of interstellar dust is less than 5%, an accurate knowledge of the instrumental polarization is mandatory for the data processing and analysis.

For this reason, we have performed a dedicated study to characterize the polarization induced within the PILOT instrument. This study comprises, in a first step, analytical calculations to evaluate the impact of each optical interface on the incident state of polarization. The results from this preliminary study are used in order to optimize a more complex model under Zemax software. The second part of the study presents a detailed Zemax modelling, aiming at predicting the instrumental polarization of the integrated instrument, for in flight and ground tests conditions. This modelling takes into account the entire field of view of the instrument (1°x1°) for several optical configurations (8 positions of the half wave-plate for in flight conditions and 8 for end to end ground tests conditions). A sensitivity study has been derived too, in order to estimate deviations from nominal instrumental polarization, for each mechanical and optical tolerance range. A synthesis of this study is presented in this article and is extensively described in [2] and [3].

B. Instrument overview

In order to reach high sensitivity, a stratospheric platform and bolometer arrays are required. For sky survey, the azimuth scanning and elevation range will be respectively ±30° and from 20° to 60°. The reconstruction of the fine attitude and effective pointing direction will be done using a stellar sensor co-aligned with the submillimeter axis (amplitude error of 10" on the three axis).

The optical design, presented on Fig. 1, comprises an off axis Gregorian telescope, a telecentric re-imaging system and a polarimeter (half wave-plate and polarizer grid). The telescope respects the Mizuguchi Dragone condition, in order to limit instrumental polarization and straylight [4]. The principle of the polarization measurement uses a design based on a rotated half-wave plate and a fixed grid polarizer. The rotation of the half-wave plate is done by discrete steps to avoid modulation of the background. Several scans are done for the same region using different wave plate angles, allowing to determine successively I and U, I and Q Stokes parameters.

All optical elements, except the primary mirror, are cooled at cryogenic temperature (about 3K), in order to reduce the instrumental background. The two focal planes are composed of four bolometer arrays, 2 per wavelength channel, cooled at 300 mK. Each array is composed of 16x16 pixels (each pixel size ~ 750 µm²), so there is a total of 2048 bolometers. An internal source of calibration is used to perform in flight inter calibration. More details on this optical concept, its performances and on the scientific instrument are given in [1], [5] and [6].

II. PRELIMINARY STUDY:

The preliminary study has been done analytically to estimate consistent hypothesis to be used in a Zemax instrument polarization modelling. For this study, we consider each type of interface with simple hypothesis: plane interfaces and one ray with various angles of incidence (from normal incidence to maximum angle of

---

[1] Polarized Instrument for Long wavelength Observation of the Tenuous interstellar medium

incidence used in the PILOT instrument). We present in this part a synthesis of the results obtained with this preliminary study. The main reference used for the calculations done in this preliminary study is [7].
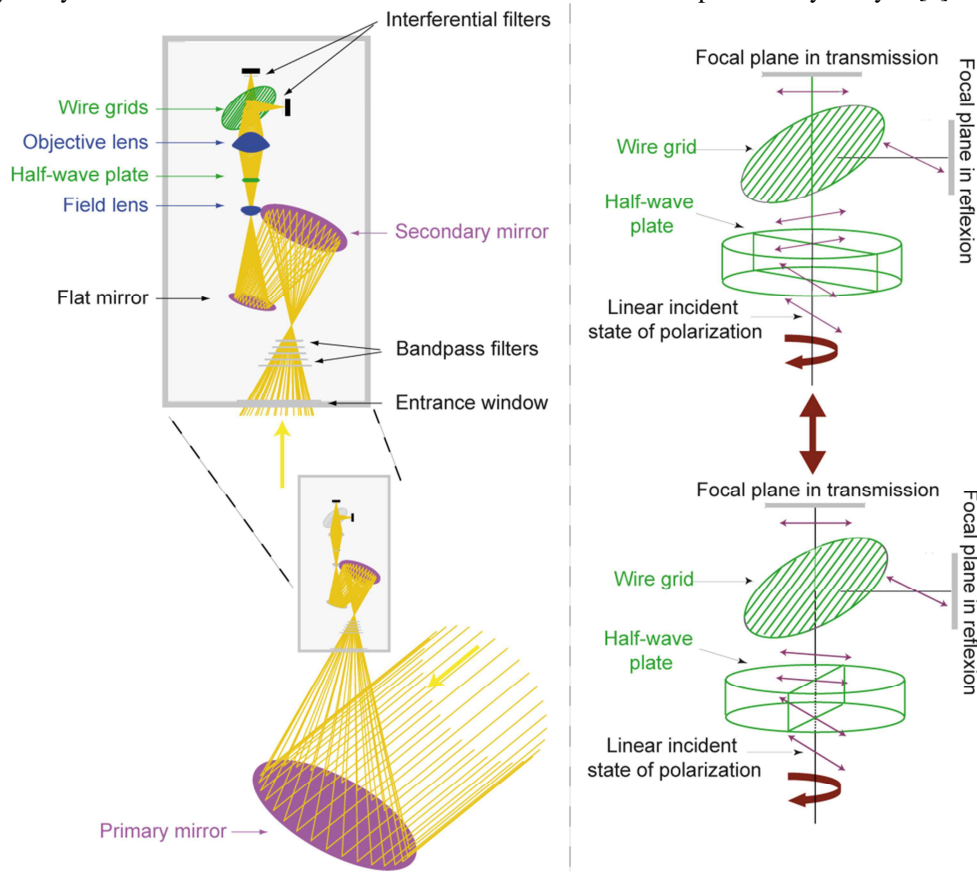

Fig. 1 Left: Schematic view of the optical system including an off axis Gregorian telescope (in purple), a telecentric re-imaging system (in blue) and a polarimeter (in green); Right: principle of the polarization measurement based on a minimum of two half-wave plate positions

A. Case of mirrors

PILOT mirrors are made of aluminum with a SiO_2 protective coating. Aluminum index is known only up to 200 µm [8]. Using Fresnel coefficient and considering that aluminum acts like a perfect reflector for long wavelength, we can estimate that the reflection coefficient is around 0.995 at PILOT wavelength. Similar calculations, considering both the aluminum substrate and the SiO_2 protective coating, show that the effect of the protective layer can be neglected.

Worst cases for rotation of plane of polarization and ellipticity are obtained when the incident state of polarization is tilted by 45° around the plane of incidence with a maximum value respectively of $1.25.10^{-3}$ and 0.03° (Fig. 2). As the metallic media of the mirrors has very little impact on ellipticity, it is then possible to model mirrors using only the reflection coefficient.
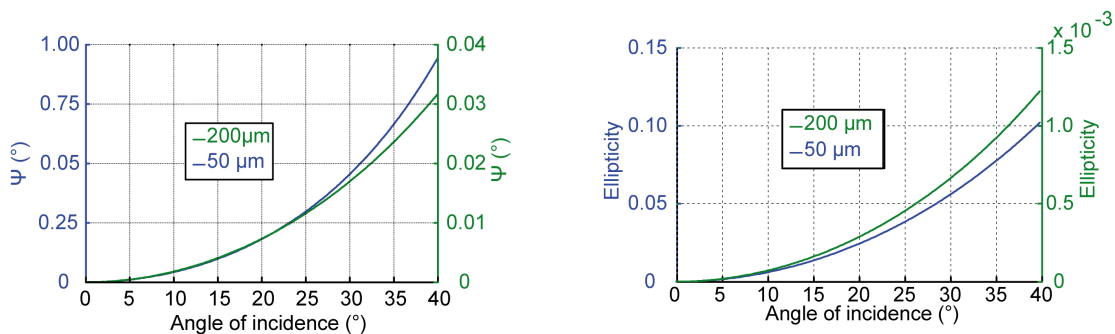

Fig. 2 Rotation of the polarization plane (left) and ellipticity (right) and as a function of the angle of incidence, incident state of polarization is linear and tilted by 45° around the plane of incidence, calculations done at 50 and 200 µm.

B.   Case of Lenses

Lenses are made of polypropylene with polytetrafluoroethylene antireflective layer. The index of these media are the same at the two PILOT wavelengths with n_s=1.52 for polypropylene (measurement done by the project team) and n_{arc}=1.4 [9].

As the index of polypropylene and polytetrafluoroethylene are real, the lenses induce no ellipticity on linear incident state of polarization. The rotation of the plane of polarization is shown on Fig. 3, for front and back side of the lenses. The rotation is less than 0.5° for front side and less than 0.25° for back side if we consider lenses with antireflection coating. Without taking into account this coating, these maximum values are multiplied by a factor 2.

The thickness of the antireflective layer is not accurately known, so we choose to consider in the Zemax model the worst case, ie lenses without antireflection coating which induce higher rotation of the plane of polarization.
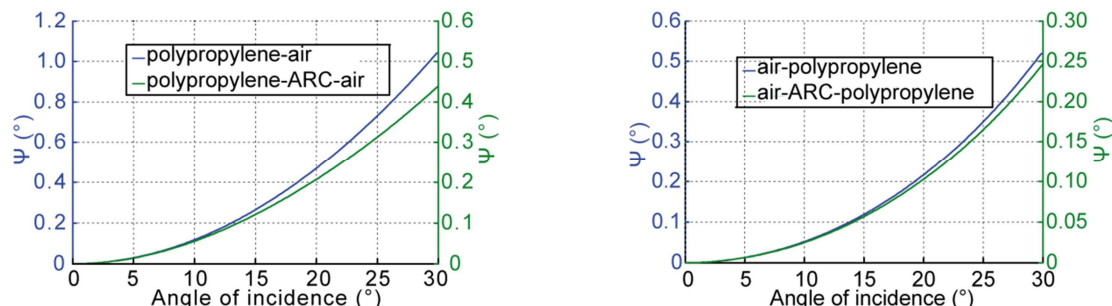

Fig. 3 Rotation of the polarization plane for back side (left) and front side (right) of a lens, as a function of the angle of incidence, corresponding to an incident state of polarization inclined by 45° in the plane of incidence, and calculations done at 240 µm with and without taking into account the antireflective layer

C.   Case of half-wave plate

The half-wave plate is made of sapphire. The ordinary indexes of sapphire are n_o=3.089 and n_o=3.084, respectively at 240 and 550 µm [4]. The extraordinary indexes are n_e=3.423 and n_e=3.415, respectively at 240 and 550 µm. As phase shift induces by the birefringent media at normal wavelength is a function of the ordinary index n_o and the extraordinary index n_e, it is then not possible to obtain exactly a phase shift of Π for the two wavelengths. The thickness of the wave plate is consequently calculated in order to obtain a similar phase shift for both wavelengths and as close as possible from Π. With this nominal thickness, the order of the half-wave plate is about 7 at 240 µm and 3 at 550 µm, with a common nominal phase shift of 179.1° at normal incidence.

The rotation of the plane of polarization and the ellipticity, induced by the plate, depend on:

- the amplitude Ao and Ae of the electric field, respectively along the ordinary and extraordinary axis of the plate,
- the phase shift (ϕ), induce by the plate
- the angle of incidence (θ),

Fig. 4 shows the ellipticity and azimuth induced by the plate, as a function of the half-wave plate optical axis orientation. The half wave plate induces ellipticity on a linear state of polarization with a maximum at $\Pi/2$ [Π] and minimum at 0 [Π] for any angle of incidence. Concerning the rotation of the plane of polarization, the maximum is at $\Pi/4$ [$\Pi/2$] and minimum at 0 [$\Pi/2$] for normal incidence. For non-normal incidence, the amplitude A_e is a function of the angle of incidence (θ), so the minima and maxima are depending on the angle of incidence.
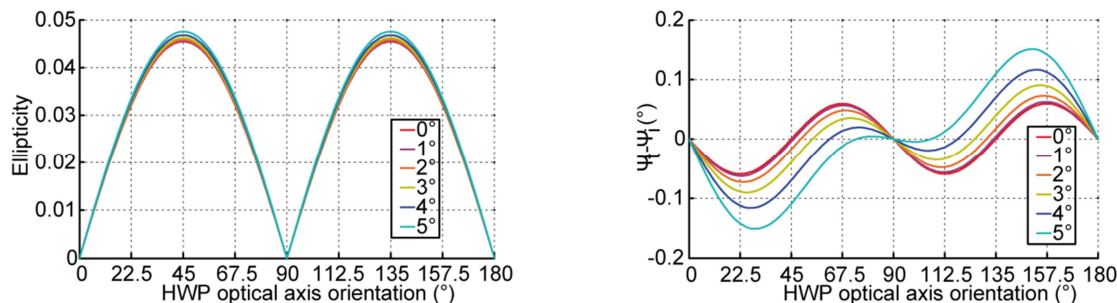

Fig. 4 Comparison of ellipticity and azimuth induced by the half-wave plate as a function of the incident state azimuth, calculations done for several angles of incidence in Oyz plane

D. Case of mesh grids: polarizer grid and mesh filters

Polarizer grid

The polarizer grid is constituted of metallic strips, regularly spaced, on a Mylar substrate. For any angle of incidence, if the space between the wires is small compared to wavelength (λ), then the transmission coefficients $T_{//}$ and $T_{\perp}$, respectively for the electrical field component parallel and perpendicular to the wires, can be estimated using [10], [11]. The reflection and transmission coefficients, as a function of the angle of incidence, are presented on Fig. 5, for PILOT parameters (a=b=5 µm). The difference between the transmission of the parallel component of the field and the reflection of the perpendicular component of the field is about 0.5% for normal incidence and 0.2% for an angle of incidence of 45° at 240 µm (average angle of incidence used in the PILOT case). The characteristics of the PILOT polarizer grid are then near a perfect polarizer.
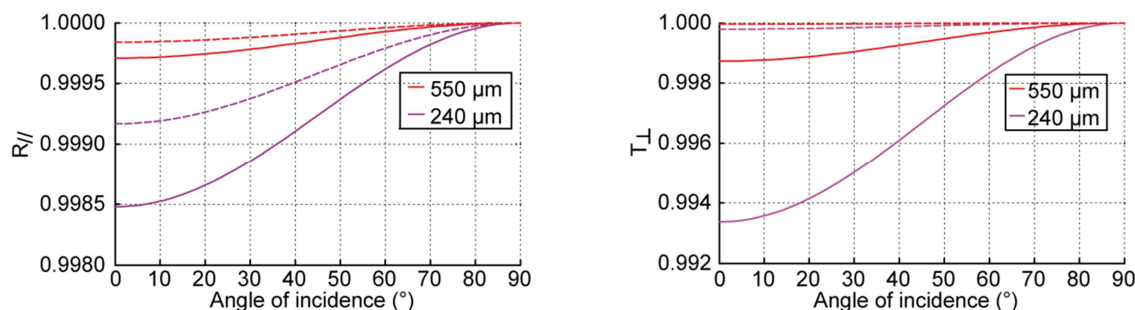
Fig. 5 Variation of the reflection coefficient (left) and of the transmission coefficient (right) as a function of the angle of incidence, respectively for the perpendicular and parallel parts of the magnetic field relatively to the wire orientation; calculation done at 240 and 550 µm, parameters for the grid is a=b=5 µm, dotted line is for air substrate, full line is for a Mylar substrate (n=1.83)

Mesh filters

Mesh filters are placed at the entrance of the cryostat (band-pass filters) and close to the bolometers arrays (interferential filters). These kinds of filters are made of several grids stacked together: 3 grids minimum are required to obtain a transmission coefficient equal to 1 (see [12], [13] and [14]). Moreover, if the distance (s) between the grids is defined by: $s=(2k-1)\lambda/4$, with k an integer, there is no rotation between the incident and transmitted state of polarization for the wavelength used for the optimization of the filter. Obviously, the hypothesis of a perfect filter transmission is valuable only for modellings done at the optimized wavelength. More complex simulations must take into account variations of transmission on the bandpass.

III. PROPAGATION OF POLARIZATION STATE IN THE OPTICAL SYSTEM:

For preliminary study, presented in II, we consider only plane interfaces and one ray for various angles of incidence. To evaluate the instrumental polarization of the entire optical system, it is mandatory to take into account the geometry of the beam and the shape of the component. In addition, the state of polarization transmitted or reflected by an optical component, is a function of the incident state of polarization. Consequently, the state of polarization analyzed by the instrument depends on the modifications induced sequentially by all the optical elements.

For this more complex study, we choose to use Zemax software, considering only one monochromatic wavelength (240 µm). Considering the results presented in II, it is obvious that modifications induced on the incident state of polarization will be maximum at this wavelength. We present in this part, the main results obtained with this Zemax modelling, using the hypothesis presented in II.

A. On the impact of the surface shape

Modifications of the state of polarization are induced by a change of medium, by the surface shape and depend also on the geometry of the incident beam. As all optical surfaces are quadratic surfaces[2], we can consider first a general quadratic surface used in reflection. We model this quadratic surface with a constant coefficient of reflection, so the results are affected only by the surface shape. Note that similar results can be obtained in transmission.

As shown on Fig. 6, for a quadratic non-metallic surface, with revolution around the optical axis Oz, the polarization states after reflection are symmetrical around Ox and Oy axis for the center of the field of view. Consequently, the resulting state of polarization doesn't rotate after reflection in this case. A similar result can be obtained for an off axis quadratic surface, as for example the red off axis surface shown on Fig. 6. In this last

---

[2] For example a plane surface is a quadratic surface with infinite radius of curvature.

case, the reflected states of polarization are symmetrical around the Oy axis and the resulting state of polarization doesn't rotate after reflection too.

This result is only valid for the center of the field of view. For other directions, the states of polarization are not symmetrical around an axis of symmetry of the quadratic surface and the resulting state of polarization rotates after reflection. This simple example shows the impact of the shape of the surface on the state of polarization and is helpful to analyze the results obtained in the Zemax modelling.
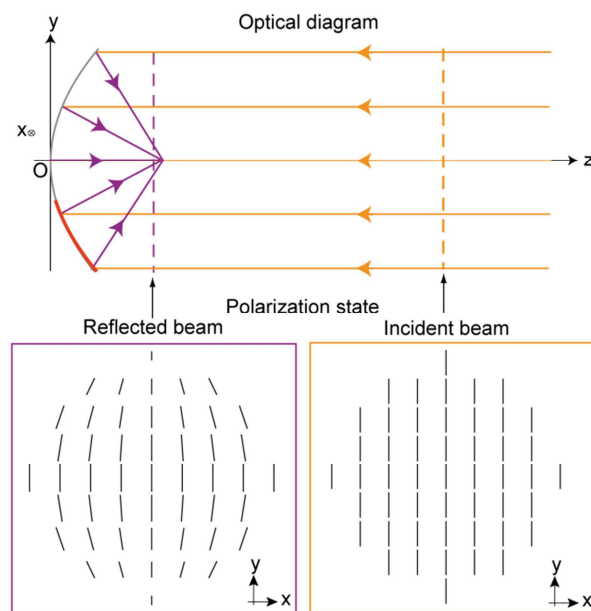

Fig. 6 Polarization states after reflection on a parabolic non-metallic mirror; the red part on the optical diagram indicates the portion of the conic corresponding to the PILOT primary mirror; case of a linear initial polarization state oriented along the Oy axis

B. On the impact of the telescope

The PILOT telescope is an off axis Gregorian type, with respect of the Mizuguchi Dragone condition. Using this condition, i.e. a combination of shape and orientation between the primary and secondary mirrors [4], the telescope properties, regarding instrumental polarization, are close to the one obtained with an on axis telescope. We first consider the telescope without taking into account the filters, located between the primary and secondary mirror, in order to evaluate the performances of the telescope configuration only. Then, we evaluate the impact of the filters on the telescope performances considering both the entrance window used for ground tests and for the flight.

Performances of the telescope configuration without taking into account the filters

For the center of the field of view, considering a linear incident state of polarization along the primary mirror axis of symmetry, the states of polarization after reflection on the mirror are symmetrical around Oy_1 axis (Fig. 7). After reflection on the secondary mirror, the states of polarization are linearly polarized along Oy_2: no modification is induced on the state of polarization by reflection on the telescope in this case.

For other fields of view, the states of polarization are slightly rotated after reflection on the telescope, as shown on Fig. 8, with a maximum rotation of 1.5° in the corner of the field of view.

Results are slightly different, if we consider linear incident states of polarization not oriented along the axis of symmetry of the primary mirror (deviation from mean value less than 0.1°). Furthermore, the telescope configuration is not very sensitive to mechanical tolerances, with a maximum variation of 0.2°, for the corner of the field of view, when the primary mirror is tilted by 0.06° around Oy.

Performances of the telescope configuration taking into account the filters

Taking into account the filters and the entrance cryostat window, placed between the primary and secondary mirror, the telescope configuration is a little less efficient. For photometry reason, the entrance window used for ground test is thicker than for flight, so we check the effect of both types of entrance windows. Considering the in-flight entrance window, the maximum rotation of the polarization plane is around 3° in the corner of the field of view. As presented in II.B., the transmission by a dielectric plane interface affects the azimuth of the state of polarization for non-normal incidence. As the beam is not symmetrical around the filters plane of incidence for every points of the field of view, the telescope performances are then affected by the filters.

We have also checked the sensitivity to optical and mechanical tolerances. Worst case is obtained for in flight configuration, when the orientation between primary and secondary mirror is tilted by 0.06°. The telescope configuration is then very poorly affected by the optical and mechanical tolerances.

The results obtained with the ground test and flight entrance windows are very similar. The telescope performances are then quite equivalent with both entrance windows.
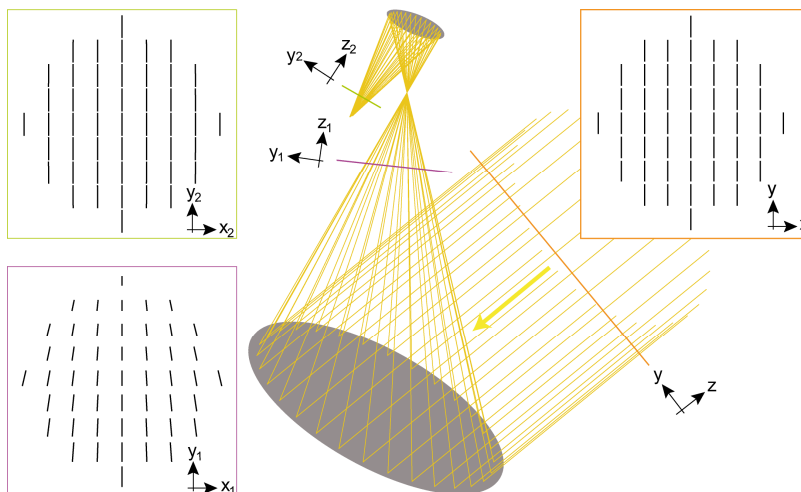

Fig. 7 State of polarization respectively after reflection on the primary mirror and the secondary mirror, with an incident beam parallel to the primary mirror optical axis; the incident polarization state is perpendicular to the incident beam and oriented following the symmetry axis of the primary mirror
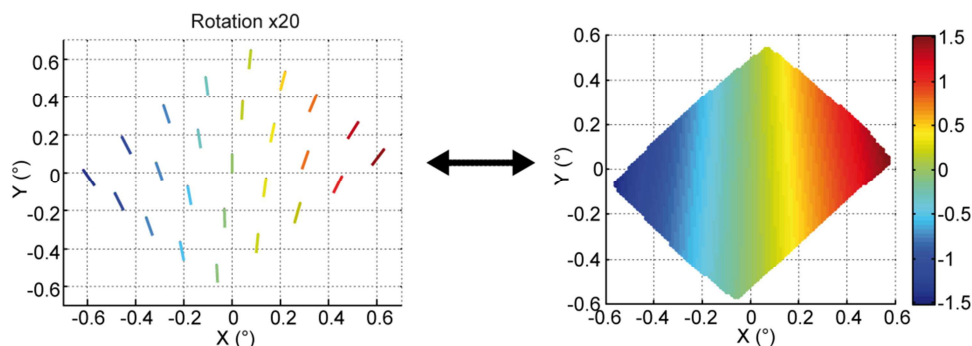

Fig. 8 Orientation of the polarization plane on the telescope focal plane, for different points of the field of view, the two figures present the same results: on the left the orientation for each point of the field of view is represented by vector with a rotation multiplied by 20 for the visual of the figure, on the right an interpolation of the results obtain on the entire field of view

C. On the impact of the reimaging system

The reimaging system is made of two on axis lenses. Consequently, for the center of the field of view, considering incident state of polarization oriented along the symmetry axis of the primary mirror, there is no rotation of the plane of polarization after transmission by lenses (Fig. 9).
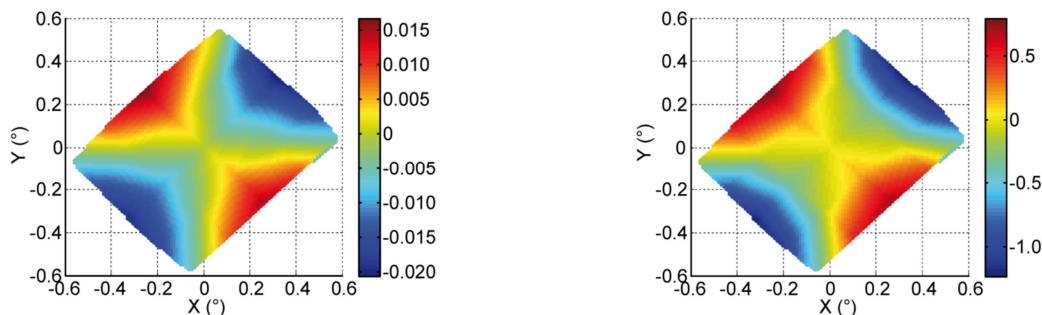

Fig. 9 Rotation of the plane of polarization for the entire field of view, induced by the objective lens (left) and by the field lens (right); the incident state of polarization is oriented along the primary mirror axis of symmetry

For other fields of view and other orientations of the incident state of polarization, the result depends on the shape of the back and front side of the lenses. As the eccentricity of the field lens is larger than for the objective lens and as the beam covers a larger part of the lens, the rotation induced by the field lens is larger than the one induced by the objective lens, with a maximum of 2° in the corner of the field of view.

These results are quite similar within the optical and mechanical tolerance ranges, with a maximum deviation of 0.03° of the plane of polarization rotation for an uncertainty of 0.1 for the front side conic constant of the objective lens.

D. On the impact of the half-wave plate

Fig. 10 shows the rotation of the plane of polarization and the ellipticity variation, induced by the half-wave plate, considering a linear incident state of polarization oriented along the primary mirror axis of symmetry. For this case, the maximum rotation of the plane of polarization and ellipticity are respectively 3° and 0.002. No modification of the state of polarization is induced by the half-wave plate for the center of the field of view. Considering any orientation of the half-wave plate optical axis, the maximum ellipticity is up to 0.075.

The results obtained, taking into account the tolerance on the half-wave plate thickness, show that the thickness tolerance has few effects on the rotation of the plane of polarization: maximum increase of 0.15° and 0.35° respectively for a decrease and an increase by 25 µm of the thickness. The ellipticity is more affected by this tolerance on thickness with an increase up to 0.18 for a thickness increase by 25 µm.

On the contrary, the system performance is robust within the tolerance range of the orientation of the half-wave plate. For a tilt of 0.1° of the optical axis of the half-wave plate relatively to the system optical axis, the rotation of the plane of polarization and ellipticity are increased respectively by 0.1° and 0.005.
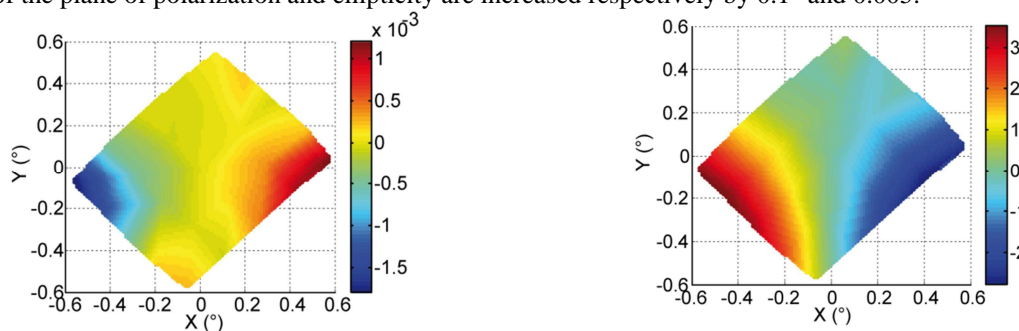

Fig. 10 Ellipticity (left) and rotation of the plane of polarization (right) for the entire field of view, after transmission by the half-wave plate, in the case of a linear incident state and optical axis of the half-wave plate-oriented along the primary mirror axis of symmetry

III. Change of polarization state induced by the whole optical system

Every component of the optical system induces alterations of the measured state of polarization. The transmitted state of polarization is then function of all modifications induced by each component and of the considered field of view. We present here, the main results obtained considering the whole optical design, except the polarizer grids, in order to well define the analyzed state of polarization.

The use of a re-imaging system allows the optimization of the image quality on the large focal plane. Consequently, the instrumental polarization is minimized too on the entire focal plane. Significant deviations are located only on the corner of the focal plane, for any orientation of the half-wave plate optical axis and linear incident state of polarization (worst case presented on Fig. 11).
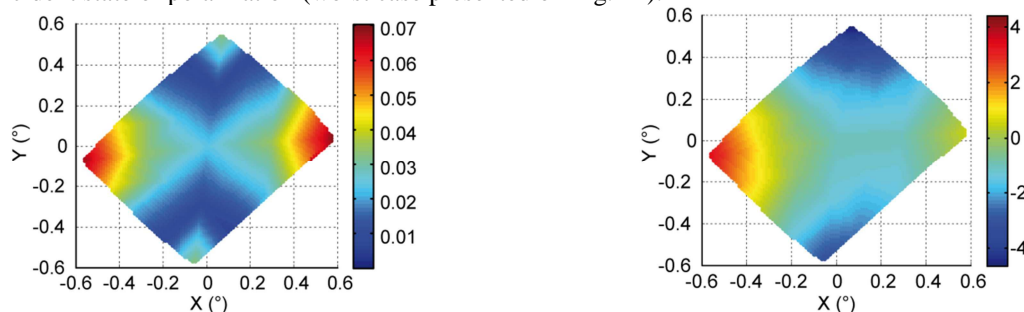

Fig. 11 Ellipticity (left) and rotation of the plane of polarization (right) induced by the instrument with flight configuration; the incident state of polarization is linear, oriented along the symmetry axis of the primary mirror, the optical axis of the half-wave plate is oriented at 45°

ICSO 2014
                               Tenerife, Canary Islands, Spain
International Conference on Space Optics
                                        7 - 10 October 2014

Maximum values of the rotation of the plane of polarization and ellipticity are respectively 4.5° and 0.075. The ellipticity is only due to the half-wave plate, and this maximum value could reach 0.18 if the half-wave plate thickness is increased by 25 µm (cf. II.C.). On the other hand, the rotation of the plane of polarization is quite similar within the optical and mechanical tolerance ranges.

The optical system is the same for in-flight and ground tests conditions, except the entrance window which is thicker for ground tests. The rotation of the plane of polarization and ellipticity, for these two configurations, are similar with a maximum difference value of respectively 0.5° and 0.01. For the center of the field of view, the deviation is less than 0.03° for the rotation of the plane of polarization and 0.001 for the ellipticity.

Considering the results presented in II and III, we can estimate that the uncertainties on the rotation of plane of polarization and the ellipticity are respectively 1° and 0.1. Consequently, we can neglect the discrepancies between these two configurations by including them in the uncertainty budget.

III. CONCLUSION AND PERSPECTIVES

This dedicated study has allowed characterizing the PILOT instrumental polarization. Our results show that it is minimized thanks to the use of the Mizuguchi Dragone condition for the telescope and the telecentricity of the reimaging system. Taking into account the uncertainty on the ellipticity and rotation of the plane of rotation, we have also shown that the instrumental polarization is similar for the flight and ground tests configurations. These results, combined with the ones obtained during end to end ground tests, will be used in the scientific data processing and analysis.

REFERENCES

[1]   J.-P. Bernard, «Dust Polarization measurements with the PILOT balloon experiment,» *39th COSPAR Scientific Assembly,* p. 150, 2012.

[2]   C. Engel, J.-P. Bernard, G. Otrio, Y. Longval, C. Marty et I. Ristorcelli, «Instrumental polarization modelling for the PILOT submm experiment,» *Experimental Astronomy,* p. unpublished, 2014.

[3]   C. Engel, «Optimisation des performances du système optique et estimation de la polarisation instrumentale de l'expérience embarquée sous ballon stratosphérique PILOT,» *PhD Thesis,* 2012.

[4]   C. Dragone, «A first-order treatment of aberrations in Cassegrainian and Gregorian,» *IEEE Transactions on Antennas and Propagation, 30,* pp. 331-339, 1982.

[5]   C. Engel, Y. Longval, J.-P. Bernard, C. Marty, G. Otrio et I. Ristorcelli, «Optical Design of the PILOT balloon borne experiment: performances and tolerances,» *Experimental Astronomy,* p. unpublished, 2014.

[6]   C. Engel, I. Ristorcelli, J. P. Bernard, Y. Longval, C. Marty, B. Mot, G. Roudil et G. Otrio, «Characterization and performances of the pimary mirror of the PILOT balloon borne experiment,» *Experimental Astronomy,* vol. 36, pp. 21-57, 2013.

[7]   M. Born et E. Wolf, «Principles of optics,» 1959.

[8]   M. A. Ordal, R. J. Bell, R. W. Alexander Jr, L. A. Newquist et M. R. Querry, «Optical properties of Al, Fe, Ti, Ta, W, and Mo at submillimeter wavelengths,» *Applied optics, 27(6),* pp. 1203-1209, 1988.

[9]   J. W. Lamb, «Miscellaneous data on materials for millimetre and submillimetre optics,» *International Journal of Infrared and Millimeter Waves,* pp. 1997-2034, 1996.

[10]   J. P. Auton, «Infrared transmission polarizers by photolithography,» *Applied optics,* pp. 1023-1027, 1967.

[11]   N. Marcuvitz, Waveguide handbook, McGraw-Hill, 1951.

[12]   L. Thourel, Calcul et conception des dispositifs en ondes centimétriques et millimétriques : Circuits passifs, Cepadues, 1988.

[13]   A. A. M. Saleh, «An adjustable Quasi-Optical Bandpass Filter-Part I : Theory and Design Formulas,» *IEEE Transactions on Microwave Theory Techniques,* vol. 22, pp. 728-734, 1974a.

[14]   A. A. M. Saleh, «An adjustable Quasi-Optical Bandpass Filter-Part II : Practical considerations,» *IEEE Transactions on Microwave Theory Techniques,* vol. 22, pp. 734-739, 1974b.